THE JOURNAL OF BIOLOGICAL CHEMISTRY VOL. 288, NO. 41, pp. 29323–29332, October 11, 2013

Silencing of Maternal Heme-binding Protein Causes Embryonic Mitochondrial Dysfunction and Impairs Embryogenesis in the Blood Sucking Insect *Rhodnius prolixus*[*]

Received for publication, August 14, 2013 Published, JBC Papers in Press, August 28, 2013, DOI 10.1074/jbc.M113.504985

Ana Beatriz Walter-Nuno[‡§], Matheus P. Oliveira[‡¶], Marcus F. Oliveira[‡¶], Renata L. Gonçalves[‡¶], Isabela B. Ramos[‡], Leonardo B. Koerich[§‖], Pedro L. Oliveira[‡§], and Gabriela O. Paiva-Silva[‡§1]

From the [‡]Instituto de Bioquímica Médica, Programa de Biologia Molecular e Biotecnologia, the [‖]Instituto de Biologia, Departamento de Genética, and the [¶]Laboratório de Inflamação e Metabolismo, Instituto Nacional de Ciência e Tecnologia de Biologia Estrutural e Bioimagem, Universidade Federal do Rio de Janeiro, Rio de Janeiro, Brazil, 21941-590 and the [§]Instituto Nacional de Ciência e Tecnologia em Entomologia Molecular, Rio de Janeiro 21941-590, Brazil

Background: *Rhodnius prolixus* presents a heme-binding protein (RHBP) in eggs and hemolymph.
Results: Eggs lacking RHBP failed to develop embryos and showed defective mitochondria.
Conclusion: Maternally provided heme transported by RHBP supports mitochondrial function and early steps of embryogenesis.
Significance: Recycling of intercellular transported heme is not restricted to heme auxotroph organisms and may be widespread in metazoans.

The heme molecule is the prosthetic group of many hemeproteins involved in essential physiological processes, such as electron transfer, transport of gases, signal transduction, and gene expression modulation. However, heme is a pro-oxidant molecule capable of propagating reactions leading to the generation of reactive oxygen species. The blood-feeding insect *Rhodnius prolixus* releases enormous amounts of heme during host blood digestion in the midgut lumen when it is exposed to a physiological oxidative challenge. Additionally, this organism produces a hemolymphatic heme-binding protein (RHBP) that transports heme to pericardial cells for detoxification and to growing oocytes for yolk granules and as a source of heme for embryo development. Here, we show that silencing of RHBP expression in female fat bodies reduced total RHBP circulating in the hemolymph, promoting oxidative damage to hemolymphatic proteins. Moreover, RHBP knockdown did not cause reduction in oviposition but led to the production of heme-depleted eggs (white eggs). A lack of RHBP did not alter oocyte fecundation. However, produced white eggs were nonviable. Embryo development cellularization and vitellin yolk protein degradation, processes that normally occur in early stages of embryogenesis, were compromised in white eggs. Total cytochrome *c* content, cytochrome *c* oxidase activity, citrate synthase activity, and oxygen consumption, parameters that indicate mitochondrial function, were significantly reduced in white eggs compared with normal dark red eggs. Our results showed that reduction of heme transport from females to growing oocytes by RHBP leads to embryonic mitochondrial dysfunction and impaired embryogenesis.

Heme is an essential molecule that plays a central role in the metabolism of all aerobic organisms. It is the prosthetic group of many hemeproteins that are involved in crucial physiological processes, such as sensing and transport of gases, energy transduction and respiration, drug detoxification, and signal transduction (1, 2). Furthermore, as a ligand it participates as a signaling molecule in the control of gene expression at different levels, including gene transcription (3), protein translation (4), sorting (5), and degradation (6, 7). However, free heme is a powerful generator of reactive oxygen species, causing oxidative damage to diverse biomolecules (8–12). Moreover, it can partition to phospholipid membranes, leading to cell disruption (13, 14). For this reason, cells strictly control heme homeostasis by regulating its biosynthesis, intra- and extracellular transport, and degradation (1).

The hematophagous insect *Rhodnius prolixus*, a vector for Chagas disease, ingests several times its own weight in blood in a single meal. Although the acquisition of host blood is essential for important physiological events, such as growth, development, and reproduction (15), digestion of hemoglobin in the intestinal lumen of these insects can lead to the formation of large amounts of free heme.

R. prolixus has several mechanisms involved in protecting against oxidative damage caused by heme (16). One of these mechanisms is *Rhodnius* heme-binding protein (RHBP),[2] a hemolymphatic protein that can bind heme molecules coming from the midgut lumen as a product of host hemoglobin digestion (17, 18). RHBP is a monomer of ~15 kDa encoded by a

* This work was supported by grants from Conselho Nacional de Desenvolvimento Científico e Tecnológico, Fundação de Coordenação de Aperfeiçoamento do Pessoal de nível Superior, Fundação de Amparo à Pesquisa de Estado do Rio de Janeiro, and the Howard Hughes Medical Institute.

[1] To whom correspondence should be addressed: Inst. de Bioquímica Médica, Programa de Biologia Molecular e Biotecnologia, Universidade Federal do Rio de Janeiro, CCS, Sala 5, Bloco D Subsolo, Ilha do Fundão, Rio de Janeiro, 21941-590, Brazil. Tel.: 55-21-25626751; Fax: 55-21-22905436; E-mail: gosilva@bioqmed.ufrj.br.

[2] The abbreviations used are: RHBP, *Rhodnius* heme-binding protein; ETS, electron transport system; 4-HNE, 4-hydroxy-2-nonenal; VT, vitellin; dsRHBP, dsRNA specific for RHBP; dsMAL, dsRNA specific for Mal.

single copy gene. Its biosynthesis occurs in all stages of insect development, exclusively in fat body. Its synthesis and secretion to hemolymphs are induced by blood ingestion. The level of RHBP mRNA reaches its peak between the second and fourth day after feeding (19). Once in the hemolymph, RHBP is taken up by growing oocytes through receptor-mediated endocytosis, lending *R. prolixus* eggs their characteristic red color. In the egg, RHBP accumulates inside the yolk granules, being degraded during embryogenesis (17, 20).

Here, we show that silencing of maternal RHBP expression leads to oxidative damage of hemolymphatic proteins and causes impairment of embryogenesis through a mechanism involving alterations in embryonic mitochondrial metabolism. The physiological role of RHBP as an essential source of heme for mitochondria function and homeostasis in the embryo is discussed.

EXPERIMENTAL PROCEDURES

Experimental Insects—Insects were taken from a colony of *R. prolixus* maintained at 28 °C and 80–90% relative humidity under a photoperiod of 12 h of light/12 h of dark. The animals used in this work were mated females fed on rabbit blood at 3-week intervals. *R. prolixus* females injected with dsRNA were kept in individual vials maintained at the same conditions. After receiving a blood meal, oviposition was followed for 21 days, the eggs laid were collected daily, and eclosion of first stage nymphs was monitored for the following 30 days.

Ethics Statement—All animal care and experimental protocols were conducted following the guidelines of the institutional care and use committee (Committee for Evaluation of Animal Use for Research from the Federal University of Rio de Janeiro), which are based on the National Institutes of Health Guide for the Care and Use of Laboratory Animals (ISBN 0-309-05377-3). The protocols were approved by the Committee for Evaluation of Animal Use for Research from the Federal University of Rio de Janeiro under registry number IBQM001. Technicians dedicated to the animal facility at the Institute of Medical Biochemistry (Federal University of Rio de Janeiro) carried out all aspects related to rabbit husbandry under strict guidelines to ensure careful and consistent handling of the animals.

Tissue Isolation and RNA Extraction—Fat bodies from fed females were dissected at different days after feeding. Total RNA was extracted from individual tissues using TRIzol reagent (Invitrogen) according to the manufacturer's instructions. RNA concentrations were determined spectrophotometrically at 260 nm on a Nanodrop 1000 spectrophotometer v.3.7 (Thermo Fisher Scientific). Following treatment with RNase-free DNaseI (Fermentas International Inc., Burlington, Canada), 1 μg of RNA was used for cDNA synthesis with a high capacity cDNA reverse transcription kit (Applied Biosystems, Foster City, CA) and random hexamers according to the manufacturer's instructions.

dsRNA Synthesis and Gene Silencing Assays—A RHBP gene fragment (450 bp) was amplified by PCR using fat bodies cDNA samples produced as described above under the following conditions: one cycle for 10 min at 95 °C, followed by forty cycles of 15 s at 95 °C, 15 s at 63 °C, and 1 min at 72 °C, with a final step of 10 min at 72 °C. The primers used were RNAiRHBPF (5′-TAATACGACTCACTATAGGGTCCTTCACAGTCTCCGGAAC-3′) and RNAiRHBPR (5′-TAATACGACTCACTATAGGGGGGTCTGGTGAAAGCACAAC-3′). These primers contained a T7 polymerase binding sequence, required for dsRNA synthesis. Amplified RHBP cDNA was used as a template for RHBP dsRNA synthesis using a MEGAScript® RNAi kit (Ambion Inc., Austin, TX) according to the manufacturer's instructions. The maltose-binding protein (MAL) gene from *Escherichia coli* (gene identifier 7129408) ligated in a pBlueScript KS+ (Stratagene) was amplified by PCR using T7 minimal promoter primers under the following conditions: one cycle for 10 min at 95 °C, followed by forty cycles of 15 s at 95 °C, 15 s at 45 °C, and 45 s at 72 °C, with a final step of 10 min at 72 °C. The PCR product produced was used as a template for Mal dsRNA synthesis as a control in the silencing assays. Following *in vitro* synthesis, both dsRNAs were purified according to the manufacturer's instructions. For RHBP silencing, 1 μg of dsRNA specific for RHBP (dsRHBP) or for Mal (dsMAL) was injected into starved insect hemocoele. Twenty-four hours after injection, the insects were fed on rabbit blood. At different days after feeding, fat bodies were dissected, total RNA was extracted, and gene silencing efficiency was evaluated by quantitative RT-PCR.

Quantitative RT-PCR Assays—Quantitative PCR was performed in a 7500 real time PCR system (Applied Biosystems) using SYBR Green PCR Master Mix (Applied Biosystems) under the following conditions: one cycle for 10 min at 95 °C, followed by fifty cycles of 15 s at 95 °C and 45 s at 60 °C. PCR amplification was performed using the following primers: qRHBPF (5′-TCCTTCACACTCTCCGCAAC-3′) (forward) and qRHBPR (5′-GTACGCTTGGTACGCCACTT-3′) (reverse). Three independent biological replicates were conducted, and all PCRs were performed in triplicate. *R. prolixus* actin gene (accession number EU2337941) expression was used as an internal control for normalization. Primers used for actin PCR amplification were RpActRT F (5′-CCATGTACCCAGGTATTGCT-3′) (forward) and RpActRT R (5′-ATCTGTTGGAAGGTGGACAG-3′) (reverse). $\Delta\Delta Ct$ values were calculated from *Ct* (cycle threshold) values obtained on quantitative RT-PCR and were used to calculate relative expression and perform statistical analysis (20). Differences were considered significant when $p < 0.05$. The relative expression values based on $2\text{-}\Delta\Delta Ct$ were used only for graphic construction. All statistical analyses were performed using Prism 4.0 software (GraphPad Software, San Diego, CA).

Detection of de Novo RHBP Protein Synthesis and Secretion—Fat bodies were dissected at different days after feeding, washed in PBS (10 mM sodium phosphate, pH 7.4, 0.15 M NaCl), and incubated in DMEM (Sigma-Aldrich) for 2 h at 28 °C (10 organs in 250 μl of medium). The supernatant was collected and centrifuged at 12,000 $\times$ *g* for 10 min at 4 °C. Media samples containing secreted proteins (30 μg) were subjected to 15% SDS-PAGE analysis (21). Proteins were transferred to a nitrocellulose membrane in 25 mM Tris, 192 mM glycine, and 20% methanol (pH 8.3) for 120 min at 70 V. Nonspecific sites were blocked with 5% nonfat milk in TBS (10 mM Tris-HCl, pH 8.0, 0.15 M NaCl) containing 0.1% Tween 20 (pH 7.4) (TBST), for

18 h at 4 °C. After washing three times with TBST with 5% nonfat milk, the blots were incubated for 2 h at room temperature with rabbit anti-RHBP antiserum (1/5,000 in TBST with 5% nonfat milk) and washed three times with TBST. After incubation with IgG anti-rabbit IgG conjugated to horseradish peroxidase diluted 1:10,000 in TBST, the membranes were washed three times with TBST and analyzed for peroxidase activity using an ECL Western blotting detection system (Thermo Scientific) according to the manufacturer's instructions. This analysis was followed by visualization on x-ray film (Amersham Biosciences). Antiserum against RHBP purified from dissected oocytes was produced as described (19).

Titration and Quantification of RHBP in the Hemolymph—Hemolymphs (5 μl) from dsRNAs-injected females were collected and immediately diluted in 500 μl of PBS containing 3–13 mg/ml phenylthiourea. Binding of heme to hemolymph protein was measured by progressively adding aliquots of 0.1 nmol of heme (0.1 mM hemin prepared in 0.1 N NaOH) and recording the absorption spectra after each addition using a GBC 920 UV-visible spectrophotometer (17). The absorbance at saturation point was used to calculate total RHBP based on the micromolar extinction coefficient of 0.0645 μM^{-1} cm^{-1}.

Quantification of Total Intracellular Heme Content—Fresh laid eggs ($n = 50$) were homogenized in 200 μl of PBS (pH 7.4) and centrifuged 3× for 12,000 × *g* at 4 °C. After centrifugation, 20 μl of egg homogenates were added to 480 μl of alkaline pyridine solution (20% (v/v) of 1 M NaOH, 48% (v/v) pyridine, 32% (v/v) MilliQ water), followed by vortexing. The samples were analyzed by light absorption wavelength scan between 500 and 600 nm, before and after the addition of sodium dithionite crystals (1–3 mg). 557- and 541-nm peaks were identified in the differential reduced minus oxidized spectra. The difference of absorbance between the 557-nm peak and the 541-nm valley was used to calculate heme concentration based on the millimolar extinction coefficient of 20.7 mM^{-1} cm^{-1}.

Analysis of Hemolymph and Egg Protein Profiles—Laid eggs (5–10 eggs) collected at different days after oviposition were homogenized in a Potter-Elvehjem tissue grinder in 0.2 ml of a mixture of protease inhibitors (0.05 mg/ml of soybean trypsin inhibitor, 0.05 mg/ml leupeptin, 1 mM benzamidine, and 0.01% PMSF, purchased from Sigma) in 20 mM Tris-HCl buffer (pH 7.4). Egg homogenates were centrifuged at 15,000 × *g* for 10 min at 4 °C. The floating lipids and the pellet were discarded, and the crude egg extract supernatant was used for protein profile analysis.

Hemolymph was diluted 1:1 in the same mixture of protease inhibitors used for egg homogenization plus 3–13 mg/ml phenylthiourea, 0.15 M NaCl, and 1 mM EDTA. Hemolymph samples were centrifuged at 15,000 × *g* for 5 min at room temperature, and the pellets were discarded. Egg homogenate and hemolymph supernatant were kept at -70 °C until use. Protein concentrations of egg homogenate and hemolymph were determined by the method of Lowry *et al.* (22) using bovine serum albumin as the standard. Clear supernatants (40 μg for egg homogenates and 30 μg for hemolymph samples) were subjected to electrophoresis on 15% SDS-PAGE gels with a constant voltage of 70 mV. The gels were stained with Coomassie Blue G and destained with distilled water (23).

Detection of Protein-HNE Adducts by Western Blot—To evaluate redox imbalance, hemolymph samples (30 μg of protein) from females injected with MAL or RHBP dsRNAs were submitted to SDS-PAGE electrophoresis (8%) and then transferred to nitrocellulose membranes as previously described. After blocking, membranes were incubated with anti-4-hydroxy-2-nonenal (anti-4-HNE) IgG (Abcam International Inc.) diluted 1:1,000 in blocking buffer for 2 h at room temperature with stirring. 4-HNE is a reactive α,β-unsaturated aldehyde produced by lipid peroxidation of polyunsaturated fatty acids that promotes protein carbonylation (24). The membranes were washed five times with TBST and then incubated with IgG anti-mouse IgG conjugated to alkaline phosphatase diluted 1:10,000 in TBST. The membranes were washed three times for 5 min with 10 mM Tris-HCl and 0.15 M NaCl (pH 7.6), and alkaline phosphatase activity was revealed using the Sigma Pierce® reagent as indicated in the manufacturer's instructions.

Fertilization Assay—To determine whether fertilization was occurring, a PCR was performed for Rp_14077, a male-specific DNA fragment (chromosome Y) (GenBank™ accession no. JX559072). Eggs from experimental individuals were collected and homogenized in lysis buffer (10 mM Tris-HCl, pH 8.0, 0.1 M EDTA, pH 8.0, 0.5% SDS, 20 μg of RNase) (Fermentas International Inc.) with 20 μg of proteinase K (Sigma-Aldrich) and incubated for 3 h at 50 °C. After incubation, genomic DNA was extracted twice with phenol (pH 8.0) and precipitated with 100% ethanol and 2 M ammonium acetate. Purified genomic DNA samples (1 μg) were used as templates for amplification of Rp_14077 using PCR Master Mix 2X (Fermentas International Inc.) according to the manufacturer's instructions. Primers used for this assay were Rp_14077_F (5′-TCCTCCGCCTTGCTTCTCTGT-3′) (forward) and Rp_14077_R (5′-GTGCGGGCGGTGGATTG-3′) (reverse).

Scanning Electron Microscopy—Opercula from day 0 eggs (1 h after oviposition) were carefully detached using sharp forceps and a histological blade. The eggs were then fixed by immersion in 2.5% glutaraldehyde and 4% freshly prepared formaldehyde in 0.1 M sodium cacodylate buffer (pH 7.2) for 24 h at 4 °C and post-fixed in 1% osmium tetroxide for 1 h at room temperature. The samples were washed in 0.1 M cacodylate buffer followed by dehydration in acetone (15, 30, 50, 70, and 90% and 2 × 100%), critical point drying, and coating with a 60-nm layer of gold. Images were obtained using a FEI Quanta 250 scanning electron microscope (FEI, Hillsboro, OR).

Light Microscopy and DAPI Staining—Day 0 and day 2 eggs were fixed as described above. For cryosections, the eggs were washed and incubated for 12 h in 20% sucrose in PBS and infiltrated for 96 h in increasing concentrations of optimal cutting temperature compound (Tissue-Tek®; 25, 50, 75, and 100% optimal cutting temperature compound). After freezing in liquid nitrogen, 10-μm-thick transversal sections were obtained using a cryostat and adhered to poly-L-lysine-coated glass slides. The sections were then incubated in 5 μg/μl DAPI for 30 min at room temperature and mounted in *N*-propyl gallate. Slides were observed using a Zeiss Observer Z1 fluorescence microscope equipped with a CCD camera model AxioCAM MRM using a DAPI filer set (λ_{em}, 340–380 nm; λ_{ex}, 435–485 nm).

Mitochondrial Content—Mitochondrial content was determined by measuring the activity of citrate synthase and the amount of cytochrome *c* through Western blot. Citrate synthase activity was assessed according to the method of Hansen and Sidell (25), with modifications. The reduction of 5,5′-dithiobis(2-nitrobenzoic acid) by citrate synthase was followed in a coupled reaction with coenzyme A and oxaloacetate. The reaction mixture (1 ml) containing 0.5 mM oxaloacetic acid, 0.25 mM 5,5′-dithiobis(2-nitrobenzoic acid), 0.3 mM acetyl CoA, and 75 mM Tris-HCl (pH 8.0) was incubated for 3 min at 30 °C. Subsequently, the reaction was triggered by addition of egg homogenate (30–40 μg of protein) and of isolated mitochondria. 5,5′-Dithiobis(2-nitrobenzoic acid) reduction rate was calculated from change in light absorption at 412 nm (extinction coefficient of 13.6 $mM^{-1} \cdot cm^{-1}$) and used for the determination of citrate synthase activity.

Western blots for cytochrome *c* were performed as described above, but using anti-cytochrome *c* mouse IgG (International Abcam Inc.) diluted 1:1,000 in blocking buffer as the primary antibody. After washing with blocking buffer, membranes were incubated with anti-mouse IgG conjugated to horseradish peroxidase (Sigma-Aldrich) diluted 1:10,000 under the same conditions of the previous incubation. Membranes were washed three times for 5 min with 10 mM Tris-HCl and 0.15 M NaCl (pH 7.6), and the peroxidase activity was revealed using a kit from Pierce Sigma®. Detection of actin was done using anti-β actin mouse IgG (Sigma-Aldrich) as a control for sample loading. The immunoblots were scanned with an HP Photosmart D110A scanner, and densitometry of bands was done using ImageJ 1.45s software.

Mitochondrial Isolation—Mitochondria from *Rhodnius* eggs were obtained by using a protocol adapted from sea urchin eggs available elsewhere (26). Approximately 1–2 mg of *Rhodnius* eggs were homogenized in 3 ml of isolation buffer (0.25 M sucrose, 100 mM Tris-HCl, pH 7.6, 1 mM EDTA, 240 mM KCl) containing 1× proteases inhibitor mixture at 4 °C using a Teflon glass potter. The homogenate was centrifuged 600 × *g* at 4 °C for 10 min. The supernatant was recovered and centrifuged 2,600 × *g* at 4 °C for 10 min. After that, the supernatant was centrifuged 15,000 × *g* at 4 °C for 15 min. The resulting pellet was washed, and the final pellet was suspended in 100 μl of isolation buffer.

Cytochrome c Oxidase Activity—Activity of cytochrome *c* oxidase was measured in triplicate at room temperature, in a total reaction volume of 1 ml, using a Shimadzu spectrophotometer UV-visible 2450 (Shimadzu Scientific Instruments, Tokyo, Japan). Enzyme activity was measured by following the decrease in absorbance caused by the oxidation of ferrocytochrome *c* (ϵ = 18.5 mM^{-1} cm^{-1}) (28). The reaction mixture consisted of 100 mM potassium phosphate (pH 7.4), 50 mM reduced cytochrome *c*. The reaction was initiated by the addition of freeze-thawed mitochondria (70 μg of protein), and the reduction in absorbance at 550 nm was monitored. KCN (1 mM) was added to inhibit cytochrome *c* oxidase activity, which was considered as the cyanide-sensitive rate of cytochrome *c* oxidation. The data are expressed as nmol of reduced cytochrome *c*/min/citrate synthase activity of isolated mitochondria.

Oxygen Consumption on Intact Eggs—Oxygen consumption rates of eggs laid by RHBP or Mal dsRNA-injected females were evaluated on a high resolution oxygraph (O_2-K Oroboros, Innsbruck, Austria). The oxygraph chamber was previously calibrated with 2 ml of 1× PBS at 27.5 °C. After calibration, the O_2 consumption rates of the newly laid eggs (n = 50) were monitored for 30 min at 27.5 °C by using their own endogenous substrates.

Measurement of Intracellular Adenine Nucleotide Levels—Intracellular AMP, ADP, and ATP content of eggs was analyzed by ion-paired reverse phase liquid chromatography. Newly laid eggs (30 min to 1 h after oviposition) were then homogenized with 0.5 ml of 6% trichloroacetic acid, neutralized with 1 M Tris solution, and centrifuged at 12,000 rpm for 5 min at 4 °C. Supernatant aliquots (200 μl) were analyzed by HPLC on a Supercosil LC-18 column (5 μm, 25 cm × 10 mm; Sigma-Aldrich) with a Supelguard precolumn using a LC-10AT device (Shimadzu) equipped with a diode array detector (SPDM10A). Isocratic elution was performed at a flow rate of 1 ml/min at room temperature with 50 mM KH_2PO_4 buffer (pH 6.0)/methanol (90:10) containing 4 mM tetrabutyl ammonium bromide. Adenine nucleotide levels were detected by UV absorbance at 254 nm. Standard curves of all adenine nucleotides were made, and peak areas were used to quantify the amount of dNTPs present in the egg samples. Dark red eggs used in the experiments were laid by dsMAL-injected females. The adenylate energy charge was calculated according to the following formula: Adenylate energy charge = ([ATP] + 1/2[ADP])/([ATP] + [ADP] + [AMP]).

RESULTS

RHBP Silencing Induced Oxidative Damage—Adult female insects were injected with dsRHBP or dsMAL 1 day prior to a blood meal. Fat body RHBP mRNA levels were more than 90% reduced in the dsRHBP-injected group between days 2 and 10 after blood feeding and remain significantly reduced until day 17 after the blood meal (Fig. 1*A*). The fat bodies from dsRHBP-injected females showed reduced ability to secrete RHBP *in vitro* (Fig. 1*A*, *inset*). As expected, total RHBP concentration increased in the hemolymph of control females (Fig. 1*B*). In contrast, RHBP levels progressively decreased in RHBP silenced female hemolymphs, as a result of gene silencing (Fig. 1*A*) and RHBP uptake by the early growing oocytes that is initiated in the first hours after the blood meal (20). Physiologically, RHBP is present in the hemolymph both as a non-heme apoprotein and as the heme-bound holoprotein (17). To evaluate the presence of apoRHBP, hemolymph from dsRNA-treated females was titrated by progressive additions of heme. Hemolymph from dsMAL-injected females presents a Soret peak at 412 nm, typical of heme-bound RHBP (Fig. 1*C*). Addition of heme to control hemolymph initially produced a Soret peak at 412 nm caused by binding of added heme to apoRHBP molecules (Fig. 1*D*). After saturation of the heme-binding sites, however, further additions of heme gradually shifted the Soret peak to lower wavelengths until it reached a spectrum similar to that of free heme (17, 18). Untreated hemolymph from dsRHBP-injected females presented a Soret peak at 409 nm before the titration (Fig. 1*C*), and upon the first addition of hemin (0.2 nmol), the absorption maximum was blue-shifted to

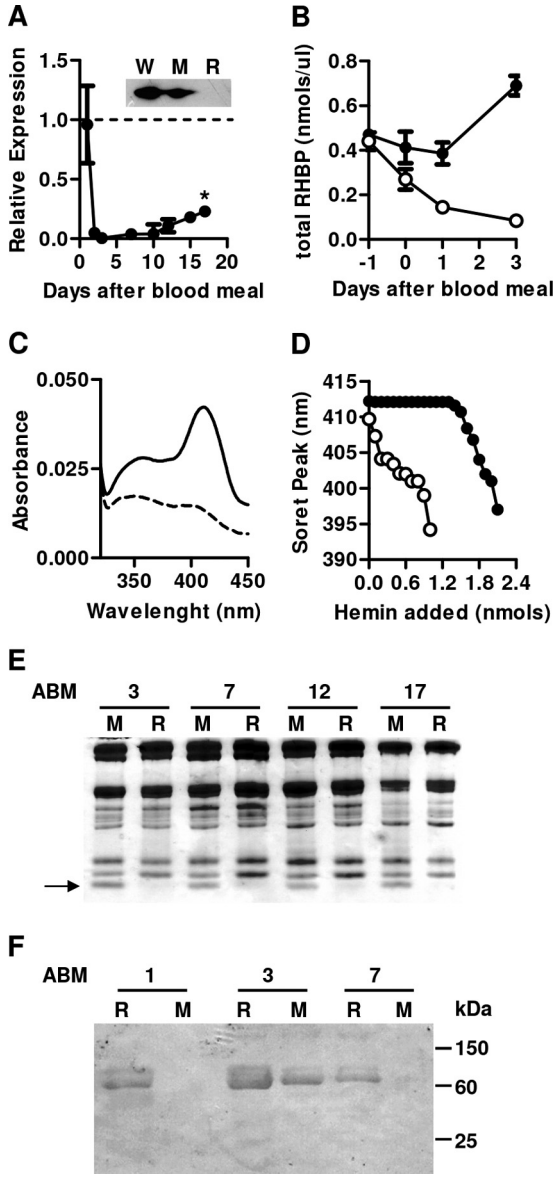

FIGURE 1. **Silencing of RHBP expression caused reduction of apo and holoRHBP levels in the hemolymph and increased oxidative damage of hemolymphatic proteins.** Adult females were injected with dsRHBP or dsMAL (control group) and fed on blood as described. *A*, quantification of *RHBP* mRNA by quantitative RT-PCR in fat bodies dissected from dsRHBP-injected females at different days after feeding. The *dashed line* represents RHBP mRNA levels of control group. The data shown are the means ± S.E. ($n = 6$). Statistical analysis was performed using analysis of variance and a posteriori Tukey's test; $p < 0.01$. *Inset*, Western blot analysis of RHBP secretion using total protein secreted by fat bodies dissected from females injected with water (*W*), dsMAL (*M*), or dsRHBP (*R*) at day 3 after feeding. The data indicate typical results of four independent experiments. *B*, RHBP concentrations in the hemolymph of dsMal (*black circles*) or dsRHBP (*open circles*) females at different days after feeding. Injections were performed 24 h before feeding (day −1). *C*, light absorption spectra of hemolymph from females injected with dsRHBP (*dashed line*) or dsMAL (*solid line*). *D*, determination of apoRHBP levels by titration of heme-binding sites in the hemolymph of silenced females. Graphic shows Soret peak shift after hemin additions to hemolymph collected from females injected with dsRHBP (*open circles*) or dsMAL (*black circles*). The results are representative of four independent experiments. *E*, 15% SDS-PAGE of hemolymphs collected on different days after feeding from females injected with dsMAL (*M*) or dsRHBP (*R*). The *numbers* indicate days after blood meal (*ABM*). The *arrow* indicates relative migration of RHBP polypeptide. Gel represents a typical result of three independent experiments. *F*, determination of oxidative damage of hemolymphatic proteins by Western blotting against 4-HNE. Hemolymphs collected on different days after feeding from females injected with dsRHBP (*R*) or dsMAL (*M*). The *numbers* indicate days after blood meal (*ABM*). The results are representative of four independent experiments.

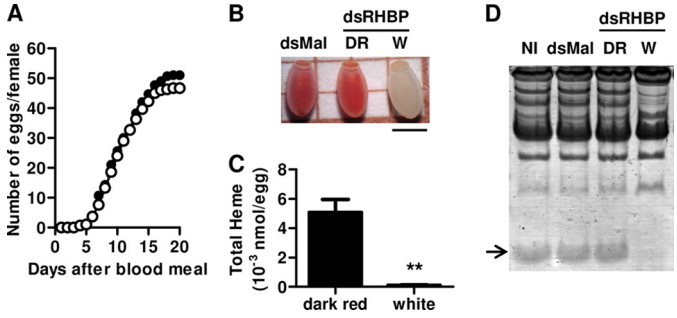

FIGURE 2. **Effect of RHBP knockdown on oviposition.** Adult females were injected with dsRHBP or dsMAL (control group) and fed on blood as described. *A*, oviposition of females injected with dsRHBP (*open circles*) or dsMAL (*black circles*) was monitored daily. The cumulative number of eggs laid is represented in the *ordinate* and corresponds to the average of eggs produced per female. Each experimental point was obtained using four pools of five females each. *B*, color pattern of dark red eggs laid by control group (dsMAL) and dark red and white eggs laid by silenced females (dsRHBP). The *bar* represents 1 mm. *C*, total heme quantification in dark red and white eggs laid by dsRHBP-injected females. *D*, 15% SDS-PAGE of egg homogenates from females injected with dsMAL, dsRHBP (dark red eggs), or dsRHBP (white eggs) or not injected (*NI*). The *arrow* indicates relative migration of RHBP polypeptide. The data indicate typical results of four independent experiments.

407 nm (Fig. 1*D*), confirming the absence of apoRHBP in silenced females. These results were further corroborated by the lack of a 15-kDa RHBP band in SDS-PAGE of hemolymph from silenced females (Fig. 1*E*).

It has already been shown that binding of heme to apoRHBP results in a markedly decreased capacity of heme for lipid peroxidation *in vitro*, suggesting that apo-RHBP could act as an antioxidant prevention mechanism in this insect (18). Here we demonstrated that RHBP had an antioxidant role *in vivo*, because hemolymph from dsRHBP-injected females presented a higher level of adducts of 4-HNE (24) on the days where RHBP expression was significantly inhibited (Fig. 1*E*). It is important to note that the insects injected with dsMAL also presented 4-HNE adduct proteins on day 3, suggesting that a basal level of oxidative damage is physiologically observed in the hemolymph of fed females on that day.

It has already been proposed that uptake of RHBP, the second most abundant yolk protein, by growing oocytes was essential for egg production (20, 27). However, the number of eggs laid by silenced insects was not significantly different from control groups (Fig. 2*A*). Instead, eggs ranging from the normal holoRHBP-containing dark red to white were laid by silenced females (Fig. 2*B*), whereas in the control groups all eggs had the regular dark red color (Table 1). RHBP knocked down females initially laid the red eggs, probably produced by the uptake of RHBP molecules synthetized before the injection of dsRHBP in the females. The following cycle of egg production generated only white eggs (data not shown). Total heme content of white eggs is highly reduced when compared with dark red eggs laid by silenced females (Fig. 2*C*). SDS-PAGE analysis of egg homogenates confirmed that white eggs, but no dark red eggs laid by silenced females, lacked RHBP (Fig. 2*D*). Most importantly, none of the white eggs laid by silenced females were viable,

TABLE 1
Phenotype and viability of eggs laid by dsRNA-injected females
The data shown are the means ± S.E. ($n = 6$) for three independent determinations.

Phenotype	White	Light red	Dark red	White	Light red	Dark red
Total eggs laid	0	0	304 ± 2.21	168 ± 3.16	38.6 ± 2.49	88.6 ± 3.30
Viable eggs	0	0	304 ± 0	0	31 ± 1.29	88.6 ± 0
Viable eggs (%)	0	0	100	0	80.31	100

whereas 81% of light red eggs and all dark red eggs were viable (Table 1).

Silencing of Maternal RHBP Impaired Embryogenesis and Caused Mitochondrial Dysfunction—Because none of the white eggs showed visible signs of embryo development, we decided to investigate whether the lack of RHBP affected fertilization and, therefore, the development of white eggs. As expected, no amplification was detected by PCR using primers for a male-specific sequence (Rp_14077) in genomic DNA samples originated from female fat body or unfertilized eggs (laid by virgin females). Conversely, DNA extracted from white or dark red eggs laid by RHBP-silenced females showed amplification of the Rp_14077 sequence, indicating that fecundation had occurred in both circumstances (Fig. 3*A*).

This result led us to further investigate the effect of RHBP deficiency on embryo development. As described by Oliveira *et al.* (28), a prominent event in *R. prolixus* embryogenesis is the limited proteolysis of vitellin (VT), the most abundant yolk protein in *R. prolixus* eggs. When analyzed by SDS-PAGE, control eggs showed progressive VT proteolysis, characterized by the disappearance of the 180-kDa VT apoprotein and the generation of fragments of lower mass (Fig. 3*B*). In contrast, VT proteolysis was completely suppressed in white eggs, indicating that embryogenesis was impaired at an early stage.

This conclusion was further supported by light and fluorescence microscopy analysis of laid eggs. Transversal sections of fertilized red eggs laid by dsMAL-injected females and white eggs from dsRHBP-silenced females showed that dsMAL embryos were in the early stages of gastrulation, as expected (29), whereas dsRHPB embryos were not formed (Fig. 3, *C–F*). No nuclei or peripheral blastodermal cells were detected after DAPI staining in dsRHBP eggs, indicating that intracellular cleavage was not triggered in zygotes from eggs lacking RHBP.

Mitochondria are key organelles in coupling energy from nutrients oxidation into ATP synthesis by means of the oxidative phosphorylation process. With a few exceptions, oxygen consumption and ATP synthesis are coupled processes and are dependent on a constant electron flow through the complexes of the so-called electron transport system (ETS). In this sense, some of the ETS redox components are in fact hemeproteins, such as cytochromes *a*, *b*, and *c.* For this reason, mitochondria are most likely the major site of heme utilization in most eukaryotic cells. Thus, shortage of heme through silencing of RHBP could affect mitochondrial physiology, potentially resulting in cellular energy failure. To address this hypothesis, egg cytochrome *c* content, an important mitochondrial protein, was determined by Western blotting. We observed that cytochrome *c* levels were lower in white eggs compared with dark red eggs, both laid by dsRHBP-injected females (Fig. 4*A*). In fact, attempts to quantify cytochromes in *Rhodnius* eggs by visible light absorption spectra were unsuccessful because of the contaminant of residual RHBP in mitochondrial preparations obtained by different methods. Indeed, the light absorption spectra of RHBP is quite similar to that of cytochrome *b* making the observation of cytochromes *b* and *c* absorption peaks very difficult (data not shown).

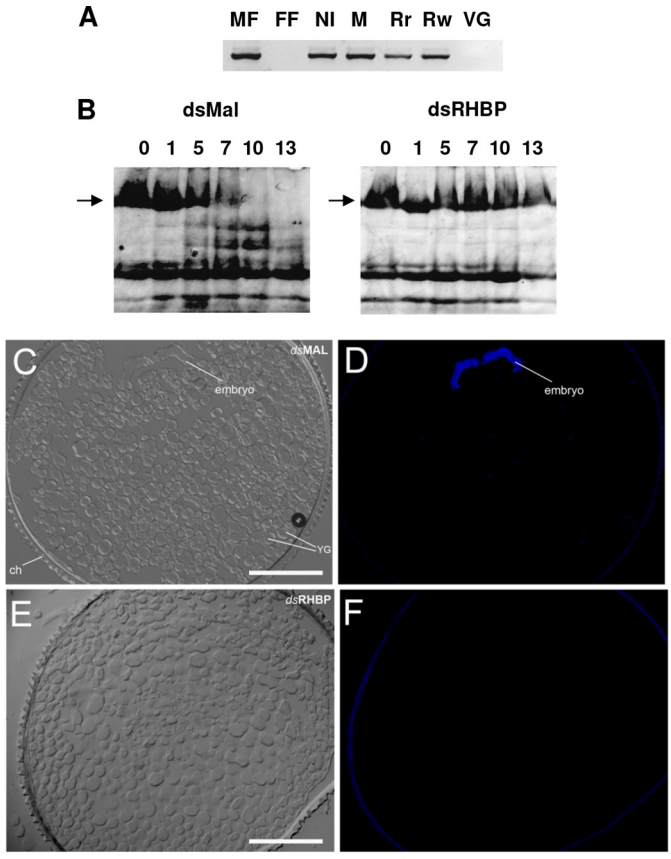

FIGURE 3. **Impairment of embryogenesis by knockdown of maternal RHBP expression.** *A*, genomic DNA from eggs laid by females injected with dsMAL (*M*), dsRHBP (*Rr*, red eggs; *Rw*, white eggs) and noninjected females (*NI*) were extracted and used as templates for amplification of a specific Y chromosome fragment by PCR. Genomic DNA from nonfertilized eggs laid by virgin females (*VG*) or from female fat body (*FF*) were used as negative controls. Male fat body DNA was used as a positive control (*MF*). *B*, embryo development monitored by degradation of vitellin, the major yolk protein. Laid eggs were collected and homogenized on consecutive days after oviposition. Total egg homogenates were then subjected to SDS-PAGE (7.5%). Typical result of three independent experiments. The *arrows* indicate relative migration of nondegraded VT (103 kDa) polypeptide. The *numbers* indicate days after oviposition. The data indicate typical results of three independent experiments. *C–F*, transversal sections of dsMAL-injected (*C* and *D*) or dsRHBP-injected (*E* and *F*) eggs fixed 3 days after oviposition and stained with DAPI (*D* and *F*). The images were obtained by differential interference contrast microscopy (*C* and *E*). Note the absence of a developing embryo in dsRHBP eggs. The *bars* represent 100 μm.

Besides cytochrome *c* content, the activity of citrate synthase, a non-heme protein, and a key enzyme in the tricarboxylic acid cycle (30) was also reduced by 37% in white eggs (Fig. 4*B*). We have also assessed the complex IV activity of the ETS, the cytochrome *c* oxidase (a cytochrome $a + a_3$ containing complex) in both white (dsRHBP) and red (dsRHBP) eggs. Fig. 4*C* shows that RHBP silencing caused a significant reduction in the cytochrome *c* oxidase activity, indicating that heme shortage affected electron delivery to oxygen by the terminal oxidase complex of the ETS. This resulted in a reduction of oxygen

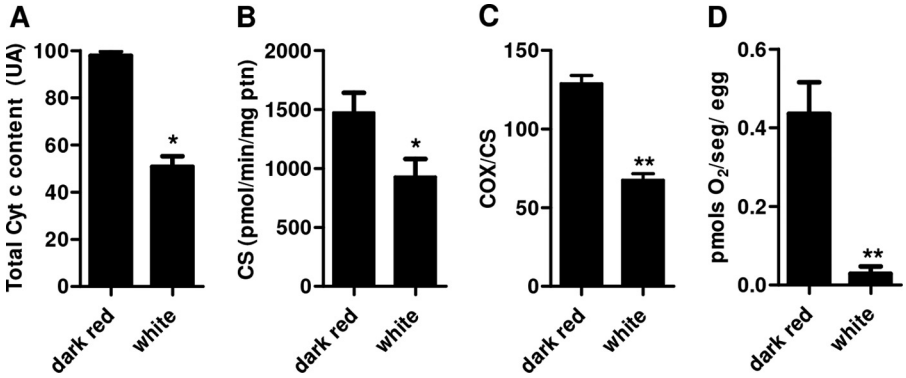

FIGURE 4. **Silencing of maternal heme-binding protein leads to mitochondrial dysfunction.** *A*, total cytochrome *c* (*Cyt c*) content of white eggs laid by silenced females compared with normal dark red eggs laid by control group (dsMAL). Egg homogenates were subjected to SDS-PAGE and Western blotting using anti-RHBP or anti-actin (loading control) antibodies. The graphic represents the quantification of the relative cytochrome *c* content determined by densitometry from four immunoblots made with different pools of five eggs each ($n = 4$ pools of 5 eggs). *, $p < 0.05$. *B*, citrate synthase (*CS*) activity of fresh egg homogenates ($n = 3$ pools of 20 eggs). *, $p < 0.05$. *C*, cytochrome *c* oxidase (*COX*) activity of isolated mitochondria, expressed as nmol of reduced cytochrome *c*/min/citrate synthase activity of isolated mitochondria ($n = 3$; **, $p < 0.01$). *D*, oxygen consumption rates of freshly laid intact eggs ($n = 3$ pools of 50 eggs). **, $p < 0.01$. The *vertical bars* represent ± S.E., and statistical analysis between the two groups was performed using Student's *t* test.

consumption in 93% in RHBP depleted eggs (Fig. 4*D*). Finally, total egg contents of ATP and ADP, but not AMP, were significantly lower in white eggs (Table 2). Interesting, nonfertilized dark red eggs had ATP and ADP levels very similar to the white eggs, but much lower than fertilized red eggs. Based on these measurements, we could estimate the adenylate energy charge of both eggs groups. In Table 2, we can observe that white eggs exhibited a dramatic reduction in adenylate energy charge, indicating that RHBP plays a key role in eggs energy homeostasis. Our data clearly indicated that reduction of heme transport from females to growing oocytes by RHBP led to embryonic mitochondrial dysfunction and impaired embryogenesis.

TABLE 2

Measurement of total adenine nucleotide levels in laid eggs

The data shown are the means ± S.E. ($n = 50$) for three independent determinations. Statistical analysis was performed using analysis of variance and a posteriori Tukey's test.

	Dark red	White	Nonfertilized
AMP (pmol/egg)	0.927 ± 0.043	1.227 ± 0.075[a]	0.878 ± 0.043
ADP (pmol/egg)	1.616 ± 0.073	0.368 ± 0.032[a]	0.529 ± 0.062[a]
ATP (pmol/egg)	7.113 ± 0.372	1.567 ± 0.224[a]	1.849 ± 0.167[a]
AEC	0.82 ± 0.001	0.55 ± 0.01[b]	0.65 ± 0.015

[a] $p < 0.05$, all relative to dark red eggs.
[b] $p = 0.027$ relative to dark red group by Kruskal-Wallis test and a posteriori Dunn's multiple comparison test.

DISCUSSION

Most eukaryotic cells are believed to synthesize their own heme, a process that is thought to be tightly coupled to the assembly of hemeproteins. The capacity of recycling heme has been described in organisms that are not able to synthesize heme, such as some pathogenic bacteria (31), Trypanosomatids (32), nematodes such as *Brugia malayi* (33) and *C. elegans* (34), and the cattle tick, *Riphicephalus microplus* (35). In the last two organisms, interorgan heme transport has been described (36, 37). Here we show, in an organism that is capable of *de novo* heme synthesis (27), that an interorgan heme transport pathway is occurring and is essential to ensure proper embryogenesis, while also driving mitochondrial appropriate biogenesis. Moreover, in addition to this role as an essential transporter of heme to the embryos, we present *in vivo* evidence showing that RHBP is also a major antioxidant in the hemolymph *in vivo*.

It has already been shown that a diet with limited heme content (females fed on plasma) (20) or inhibition of *de novo* heme biosynthesis (27) cause a reduction in oviposition in *R. prolixus*. These results led the authors to suggest that maternally derived heme is fundamental for egg production. The fact that reduced availability of hemolymphatic heme (Fig. 1, *B* and *C*) through RHBP knockdown did not affect the number of eggs laid (Fig. 2*A*) and allowed the production of white eggs (Fig. 2*B* and Table 1), indicating that heme is not essential for oocyte assembly. Instead, the maintenance of appropriate heme levels during oogenesis has been shown to be crucial for the success of embryo development afterward because all of the white eggs laid were unviable (Table 1).

Interestingly, most, but not all, light red eggs that presented lower levels of RHBP were viable (Table 1), indicating that a minimal level of heme-RHBP is sufficient for embryogenesis. It is worth noting that heme synthesis by ovaries, which is higher during intense oogenesis (27), did not prevent the formation of white eggs by females that had silenced RHBP expression. This phenomenon indicated that the major source of heme for growing oocytes was RHBP taken up by endocytosis and not from adjacent ovarian follicular cells or tropharies. Furthermore, the *de novo* heme synthesis by the embryos, which is very low before egg hatching (40), is not sufficient to assurance the initial embryogenesis steps. However, it is not clear how the different sources of heme (from maternal *de novo* synthesis in the different organs or from diet) that circulate extracellularly bound to RHBP contribute to the demand of embryos. Previous works have shown that RHBP incorporated into yolk granules during oogenesis is degraded during embryogenesis just as regular yolk protein (40). However, although RHBP levels decrease because of proteolysis, heme levels remain unchanged during embryo development. The activity of ALA-dehydratase in embryos, the second enzyme in the heme biosynthetic pathway, is very low, indicating negligible heme biosynthesis (27, 40). Furthermore, no traces of biliverdin or RpBV, a modified biliverdin produced by heme degradation in this insect (39, 40), could be found in embryos. Thus, the stability observed in heme levels during

embryogenesis could not be explained by a simple balance between heme degradation and endogenous biosynthesis pathways in embryos, as occurs in most metazoan cells (1, 41). This phenomenon indicated that RHBP is a major source of heme and not iron for embryos because heme is recycled and used for the synthesis of new embryonic hemeproteins. As mentioned above, recycling of heme has been described only in heme auxotroph animals (35, 36). The fact that *R. prolixus* embryos depend primarily on maternally provided heme molecules to complete embryogenesis suggests that the recycling of heme is a process that may be more widespread among metazoans than suspected.

Our results indicated that the availability of cytosolic heme affects the intramitochondrial heme levels, suggesting the existence of an effective heme transport system from the yolk granule, where RHBP is stored, to mitochondria in embryos. This trafficking machinery must include proteins capable of binding heme molecules released by RHBP degradation in the periphery of yolk granules and of transporting it across the cytosol to different organelles where heme is required, including mitochondria. Furthermore, proteins responsible for heme traffic across the organelle membranes and for the incorporation of heme into the target hemeproteins are also required. A set works describing inter- and intracellular heme transport systems in *C. elegans* were recently published (36, 42). The complex heme transport system involves functionally different proteins named HRG, initially identified in a screen for genes regulated by heme (43, 44). Among them, HRG-3 has been described as an extracellular heme transporter (36). RHBP and HRG-3 have no amino acid sequence homology or conserved domains, which suggests that they have no common evolutionary origin. However, comparisons between heme transport systems disclosed many similarities: both are synthesized and then secreted to the circulatory system (36, 19) to act as intercellular transport proteins, delivering heme to different tissues (36, 39). Furthermore, a high level of embryo lethality is observed among eggs laid by HRG-3 null mutant worms and ones laid by RHBP knocked down insect females (36).

Our results suggested that RHBP-deficient eggs did not complete even the very early steps of embryo development, because cellularization did not take place (Fig. 3, *C–F*). This phenotype might be directly related to heme depletion, possibly as a consequence of its function in mitochondria and the high energetic input required for the rapid cell division occurring in the beginning of embryogenesis. Actually, reduction of intracellular heme levels caused a decrease in total cytochrome *c* (Fig. 4*A*). Even more significant was that heme deprivation resulted in a global imbalance of mitochondrial physiology, affecting central mechanisms of this organelle including cytochrome *c* oxidase activity (Fig. 4*C*); energy conservation reactions, evidenced as reduced ATP levels (Table 2); and oxygen consumption (Fig. 4*D*). These observations were consistent with the fact that heme plays a key role in the ETS. Furthermore, lower activity of citrate synthase in RHBP-silenced insects may suggest that mitochondrial biogenesis was somehow compromised (Fig. 4*B*).

In addition to their major role in energy metabolism, mitochondria have been implicated in the regulation of cytosolic concentrations of calcium, including transient oscillations of intracellular Ca^{2+} levels (calcium waves) triggered by fertilization and essential for egg activation. In this case, mitochondria seemed to take part in the control of calcium homeostasis, working in coordination with the ER as a buffer of cytosolic Ca^{2+} (45, 46). It has already been shown that elevated [Ca^{2+}] in the mitochondrial matrix raises ATP production through different mechanisms (45, 47, 48) that include stimulation of substrate uptake (49) and TCA cycle (50), as well as direct priming of F_0/F_1-ATP synthase (51). Interestingly, an increase in ATP synthesis is crucial to sustain the sperm-triggered Ca^{2+} oscillations in mouse eggs, allowing embryo development (52). Altogether, these data support our observations that normal fecundated eggs had higher levels of intracellular ATP and ADP than nonfertilized eggs and significant reduction of these same adenine nucleotides in heme-depleted eggs, where mitochondrial activity is compromised (Table 2).

Conceivably the impairment of vitellin degradation observed in white eggs (Fig. 3*B*) might be explained by an imbalance of calcium homeostasis caused by mitochondrial dysfunction, because it has already been shown that yolk degradation during early embryogenesis is preceded by fusion of yolk granules. This fusion is dependent on intracellular concentrations of Ca^{2+} in insects, including *R. prolixus* (38, 53). The role of intracellular levels of heme in the maintenance of Ca^{2+} homeostasis remains to be investigated.

The role of mitochondrial function and metabolism in embryonic development has been studied in the past few years in several animal models, from worms to mammals. However, the importance of heme homeostasis in these processes during oogenesis and embryogenesis has received little attention. We believe that our data point to the existence of cross-talk between heme metabolism, mitochondrial physiology, and embryo development.

Acknowledgments—We thank J. S. Lima, Jr., L. M. Rodrigues, and S. R. de Cassia for valuable technical assistance and M. H. F. Sorgine and E. A. Machado for critical discussion and suggestions.

REFERENCES

1. Ponka, P. (1999) Cell biology of heme. *Am. J. Med. Sci.* **318,** 241–256
2. Mense, S. M., and Zhang L. (2006) Heme. A versatile signaling molecule controlling the activities of diverse regulators ranging from transcription factors to MAP kinases. *Cell Res.* **16,** 681–692
3. Ogawa, K., Sun, J., Taketani, S., Nakajima O., Nishitani, C., Sassa, S., Hayashi, N., Yamamoto, M., Shibahara, S., Fujita, H., and Igarashi, K. (2001) Heme mediates derepression of Maf recognition element through direct binding to transcription repressor Bach1. *EMBO J.* **20,** 2835–2843
4. Rafie-Kolpin, M., Chefalo, P. J., Hussain, Z., Hahn, J., Uma, S., Matts, R. L., and Chen, J. J. (2000) Two heme-binding domains of heme-regulated eukaryotic initiation factor-2α kinase. N terminus and kinase insertion. *J. Biol. Chem.* **275,** 5171–5178
5. Lathrop, J. T., and Timko, M. P. (1993) Regulation by heme of mitochondrial protein transport through a conserved amino acid motif. *Science* **259,** 522–525
6. Qi, Z., Hamza, I., and O'Brian, M. R. (1999) Heme is an effector molecule for iron-dependent degradation of the bacterial iron response regulator (Irr) protein. *Proc. Natl. Acad. Sci. U.S.A.* **96,** 13056–13061
7. Zenke-Kawasaki, Y., Dohi, Y., Katoh, Y., Ikura, T., Ikura, M., Asahara, T., Tokunaga, F., Iwai, K., and Igarashi, K. (2007) Heme induces ubiquitina-

tion and degradation of the transcription factor Bach1. *Mol. Cell Biol.* **27,** 6962–6971
8. Vincent, S. H., (1989) Oxidative effects of heme and porphyrins on proteins and lipids. *Semin. Hematol.* **26,** 105–113
9. Gutteridge, J. M., and Smith, A. (1988) Antioxidant protection by haemopexin of haem-stimulated lipid peroxidation. *Biochem. J.* **256,** 861–865
10. Aft, R. L., and Mueller, G. C. (1983) Hemin-mediated DNA strand scission. *J. Biol. Chem.* **258,** 12069–12072
11. Aft, R. L., and Mueller, G. C. (1984) Hemin-mediated oxidative degradation of proteins. *J. Biol. Chem.* **259,** 301–305
12. Tappel, A. L. (1955) Unsaturated lipid oxidation catalyzed by hematin compounds. *J. Biol. Chem.* **217,** 721–733
13. Schmitt, T. H., Frezzatti, W. A., Jr., and Schreier, S. (1993) Heme-induced lipid membrane disorder and increased permeability. A molecular model for the mechanism of cells lysis. *Arch. Biochem. Biophys.* **307,** 96–103
14. Orjih, A. U., Banyal, H. S., Chevli, R., and Fitch, C. D. (1981) Hemin lyses malaria parasites. *Science* **214,** 667–669
15. Friend, W. G., Choy, C. T., and Cartwright, E. (1965) The effect of nutrient intake on the development and the egg production of *Rhodnius prolixus* Stal. *Can. J. Zool.* **43,** 891–904
16. Graça-Souza, A. V., Maya-Monteiro, C., Paiva-Silva, G. O., Braz, G. R., Paes, M. C., Sorgine, M. H., Oliveira, M. F., and Oliveira, P. L. (2006) Adaptations against heme toxicity in blood-feeding arthropods. *Insect Biochem. Mol. Biol.* **36,** 322–335
17. Oliveira, P. L., Kawooya, J. K., Ribeiro, J. M., Meyer, T., Poorman, R., Alves, E. W., Walker, F. A., Machado, E. A., Nussenzveig, R. H., and Padovan, G. J. (1995) A heme-binding protein from hemolymph and oocytes of the blood-sucking insect, *Rhodnius prolixus*. *J. Biol. Chem.* **270,** 10897–10901
18. Dansa-Petretski, M., Ribeiro, J. M., Atella, G. C., Masuda, H., and Oliveira, P. L. (1995) Antioxidant role of *Rhodnius prolixus* heme-binding protein. Protection against heme-induced lipid peroxidation. *J. Biol. Chem.* **270,** 10893–10896
19. Paiva-Silva, G. O., Sorgine, M. H., Benedetti, C. E., Meneghini, R., Almeida, I. C., Machado, E. A., Dansa-Petretski, M., Yepiz-Plascencia, G., Law, J. H., Oliveira, P. L., and Masuda, H. (2002) On the biosynthesis of *Rhodnius prolixus* heme-binding protein. *Insect Biochem. Mol. Biol.* **32,** 1533–1541
20. Machado, E. A., Oliveira, P. L., Moreira, M. F., de Souza, W., and Masuda, H. (1998) Uptake of *Rhodnius* heme-binding protein (RHBP) by the ovary of *Rhodnius prolixus*. *Arch. Insect Biochem. Physiol.* **39,** 133–143
21. Laemmli, U. K. (1970) Cleavage of structural proteins during the assembly of the head of bacteriophage T4. *Nature* **227,** 680–685
22. Lowry, O. H., Rosebrough N. J., Farr A. L., and Randall R. J. (1951) Protein measurement with the Folin phenol reagent. *J. Biol. Chem.* **193,** 265–275
23. Neuhoff, V., Arold, N., Taube, D., and Ehrhardt, W. (1988) Improved staining of proteins in polyacrylamide gels including isoelectric focusing gels with clear background at nanogram sensitivity using Coomassie Brilliant Blue G-250 and R-250. *Electrophoresis* **9,** 255–262
24. Uchida, K., Szweda, L. I., Chae, H. Z., and Stadtman, E. R. (1993) Immunochemical detection of 4-hydroxynonenal protein adducts in oxidized hepatocytes. *Proc. Natl. Acad. Sci. U.S.A.* **90,** 8742–8746
25. Hansen, C. A., and Sidell, B. D. (1983) Atlantic hagfish cardiac muscle. Metabolic basis of tolerance to anoxia. *Am. J. Physiol.* **244,** R356–R362
26. Cantatore, P., Nicotra, A., Loria, P., and Saccone, C. (1974) RNA synthesis in isolated mitochondria from sea urchin embryos. *Cell Differ.* **3,** 45–53
27. Braz, G. R., Abreu, L., Masuda, H., and Oliveira, P. L. (2001) Heme biosynthesis and oogenesis in the blood-sucking bug, *Rhodnius prolixus*. *Insect Biochem. Mol. Biol.* **31,** 359–364
28. Oliveira, P. L., Petretski, M. D., and Masuda, H. (1989) Vitellin processing and degradation during embryogenesis in *Rhodnius prolixus*. *Insect Biochem.* **19,** 489–498
29. Kelly, G. M., and Huebner, E. (1989) Embryonic development of the hemipteran insect *Rhodnius prolixus*. *J. Morphol.* **199,** 175–196
30. Larsen, S., Nielsen, J., Hansen, C. N., Nielsen, L. B., Wibrand, F., Stride, N., Schroder, H. D., Boushel, R., Helge, J. W., Dela, F., and Hey-Mogensen, M. (2012) Biomarkers of mitochondrial content in skeletal muscle of healthy young human subjects. *J. Physiol.* **590,** 3349–3360
31. White, D. C., and Granick, S. (1963) Hemin biosynthesis in *Haemophilus*. *J. Bacteriol.* **85,** 842–850
32. El-Sayed, N. M., Myler, P. J., Blandin, G., Berriman, M., Crabtree, J., Aggarwal, G., Caler, E., Renauld, H., Worthey, E. A., Hertz-Fowler, C., Ghedin, E., Peacock, C., Bartholomeu, D. C., Haas, B. J., Tran, A. N., Wortman, J. R., Alsmark, U. C., Angiuoli, S., Anupama, A., Badger, J., Bringaud, F., Cadag, E., Carlton, J. M., Cerqueira, G. C., Creasy, T., Delcher, A. L., Djikeng, A., Embley, T. M., Hauser, C., Ivens, A. C., Kummerfeld, S. K., Pereira-Leal, J. B., Nilsson, D., Peterson, J., Salzberg, S. L., Shallom, J., Silva, J. C., Sundaram, J., Westenberger, S., White, O., Melville, S. E., Donelson, J. E., Andersson, B., Stuart, K. D., and Hall, N. (2005) Comparative genomics of trypanosomatid parasitic protozoa. *Science* **309,** 404–409
33. Ghedin, E., Wang, S., Spiro, D., Caler, E., Zhao, Q., Crabtree, J., Allen, J. E., Delcher, A. L., Guiliano, D. B., Miranda-Saavedra, D., Angiuoli, S. V., Creasy, T., Amedeo, P., Haas, B., El-Sayed, N. M., Wortman, J. R., Feldblyum, T., Tallon, L., Schatz, M., Shumway, M., Koo, H., Salzberg, S. L., Schobel, S., Pertea, M., Pop, M., White, O., Barton, G. J., Carlow, C. K., Crawford, M. J., Daub, J., Dimmic, M. W., Estes, C. F., Foster, J. M., Ganatra, M., Gregory, W. F., Johnson, N. M., Jin, J., Komuniecki, R., Korf, I., Kumar, S., Laney, S., Li, B. W., Li, W., Lindblom, T. H., Lustigman, S., Ma, D., Maina, C. V., Martin, D. M., McCarter, J. P., McReynolds, L., Mitreva, M., Nutman, T. B., Parkinson, J., Peregrín-Alvarez, J. M., Poole, C., Ren, Q., Saunders, L., Sluder, A. E., Smith, K., Stanke, M., Unnasch, T. R., Ware, J., Wei, A. D., Weil, G., Williams, D. J., Zhang, Y., Williams, S. A., Fraser-Liggett, C., Slatko, B., Blaxter, M. L., and Scott, A. L. (2007) Draft genome of the filarial nematode parasite *Brugia malayi*. *Science* **317,** 1756–1760
34. Rao, A. U., Carta, L. K., Lesuisse, E., and Hamza, I. (2005) Lack of heme synthesis in a free-living eukaryote. *Proc. Natl. Acad. Sci. U.S.A.* **102,** 4270–4275
35. Braz, G. R., Coelho, H. S., Masuda, H., and Oliveira, P. L. (1999) A missing metabolic pathway in the cattle tick *Boophilus microplus*. *Curr. Biol.* **9,** 703–706
36. Chen, C., Samuel, T. K., Sinclair, J., Dailey, H. A., and Hamza, I. (2011) An intercellular heme-trafficking protein delivers maternal heme to the embryo during development in *C. elegans*. *Cell* **145,** 720–731
37. Maya-Monteiro, C. M., Daffre, S., Logullo, C., Lara, F. A., Alves, E. W., Capurro, M. L., Zingali, R., Almeida, I. C., and Oliveira, P. L. (2000) HeLp, a heme lipoprotein from the hemolymph of the cattle tick, *Boophilus microplus*. *J. Biol. Chem.* **275,** 36584–36589
38. Ramos, I. B., Miranda, K., De Souza, W., and Machado, E. A. (2006) Calcium-regulated fusion of yolk granules during early embryogenesis of *Periplaneta americana*. *Mol. Reprod. Dev.* **73,** 1247–1254
39. Paiva-Silva, G. O., Cruz-Oliveira, C., Nakayasu, E. S., Maya-Monteiro, C. M., Dunkov, B. C., Masuda, H., Almeida, I. C., and Oliveira, P. L. (2006) A heme-degradation pathway in a blood-sucking insect. *Proc. Natl. Acad. Sci. U.S.A.* **103,** 8030–8035
40. Braz, G. R., Moreira, M. F., Masuda, H., and Oliveira, P. L. (2002) *Rhodnius* heme-binding protein (RHBP) is a heme source for embryonic development in the blood-sucking bug *Rhodnius prolixus* (Hemiptera, Reduviidae). *Insect Biochem. Mol. Biol.* **32,** 361–367
41. Hamza, I., and Dailey, H. A. (2012) One ring to rule them all. Trafficking of heme and heme synthesis intermediates in the metazoans. *Biochim. Biophys. Acta* **1823,** 1617–1632
42. Chen, C., Samuel, T. K., Krause, M., Dailey, H. A., and Hamza I. (2012) Heme utilization in the *Caenorhabditis elegans* hypodermal cells is facilitated by heme-responsive gene-2. *J. Biol. Chem.* **287,** 9601–9612
43. Rajagopal, A., Rao, A. U., Amigo, J., Tian, M., Upadhyay, S. K., Hall, C., Uhm, S., Mathew, M. K., Fleming, M. D., Paw, B. H., Krause, M., and Hamza, I. (2008) Haem homeostasis is regulated by the conserved and concerted functions of HRG-1 proteins. *Nature* **453,** 1127–1131
44. Severance, S., Rajagopal, A., Rao, A. U., Cerqueira, G. C., Mitreva, M., El-Sayed, N. M., Krause, M., and Hamza, I. (2010) Genome-wide analysis reveals novel genes essential for heme homeostasis in *Caenorhabditis elegans*. *PLoS Genet.* **6,** e1001044
45. Dumollard, R., Duchen, M., and Sardet, C. (2006) Calcium signals and mitochondria at fertilisation. *Semin. Cell Dev. Biol.* **17,** 314–323
46. Miao, Y. L., and Williams, C. J. (2012) Calcium signaling in mammalian egg activation and embryo development. The influence of subcellular localization. *Mol. Reprod. Dev.* **79,** 742–756

47. Jouaville, L. S., Pinton, P., Bastianutto, C., Rutter, G. A., and Rizzuto, R. (1999) Regulation of mitochondrial ATP synthesis by calcium. Evidence for a long-term metabolic priming. *Proc. Natl. Acad. Sci. U.S.A.* **96,** 13807–13812
48. Duchen, M. R., Verkhratsky, A., and Muallem, S. (2008) Mitochondria and calcium in health and disease. *Cell Calcium* **44,** 1–5
49. Satrústegui, J., Pardo, B., and Del Arco, A. (2007) Mitochondrial transporters as novel targets for intracellular calcium signaling. *Physiol. Rev.* **87,** 29–67
50. McCormack, J. G., Halestrap, A. P., and Denton, R. M. (1990) Role of calcium ions in regulation of mammalian intramitochondrial metabolism. *Physiol. Rev.* **70,** 391–425
51. Territo, P. R., Mootha, V. K., French, S. A., and Balaban, R. S. (2000) Ca^{2+} activation of mitochondrial oxidative phosphorylation. Role of the F_0/F_1-ATPase. *Am. J. Physiol. Cell Physiol.* **278,** C423–C435
52. Dumollard, R., Marangos, P., Fitzharris, G., Swann, K., Duchen, M., and Carroll, J. (2004) Sperm-triggered [Ca^{2+}] oscillations and Ca^{2+} homeostasis in the mouse egg have an absolute requirement for mitochondrial ATP production. *Development.* **131,** 3057–3067
53. Ramos, I. B., Miranda, K., de Souza, W., Oliveira, D. M., Lima, A. P., Sorgine, M. H., and Machado, E. A. (2007) Calcium-regulated fusion of yolk granules is important for yolk degradation during early embryogenesis of *Rhodnius prolixus* Stahl. *J. Exp. Biol.* **210,** 138–148